version 1.0: May 28, 2006 DØ note 5126 - conf
comment to d0-run2eb-014@fnal.gov
primary author: Vincent LESNÉ

Search for the associated production of charginos and neutralinos in like sign dimuon channel

The DØ collaboration

Contact person: Vincent LESNÉ (lesne@fnal.gov)

Abstract

A search for the associated production of charginos and neutralinos has been performed in $p\bar{p}$ collisions recorded with the DØ detector at a center of mass energy of 1.96 TeV at the Tevatron collider. Final state with two like sign muons and missing transverse energy is under consideration. A dataset corresponding to an integrated luminosity of 902 pb^{-1} has been analyzed and limits on $\sigma(p\bar{p} \rightarrow \widetilde{\chi}_1^{\pm}\widetilde{\chi}_2^0) \times BR(3\ell)$ have been set.

Preliminary results for summer 2006 conferences

1 Introduction

Supersymmetry is a proposed symmetry relating bosonic and fermionic states [1]. The minimal extension of the standard model including supersymmetry is the minimal supersymmetric standard model (MSSM) [2]. In the theorical framework of the MSSM, the existence of a supersymmetric partner (called sparticle) for each standard model particle is postulated. Only the lightest sparticles may be observable at the Tevatron energy scale. In the mSUGRA supersymmetry breaking scenario [3], neutralinos and charginos, which are a mixing of the superpartners of the electroweak gauge bosons and the Higgs bosons, are considered promising candidates for a discovery at the Tevatron. In such a R-parity conserved theory [4], sparticles are pair produced from p$\bar{\text{p}}$ collisions and the lightest supersymmetric particle (LSP), which is stable, escapes detection leading to a significant amount of missing transverse energy. The associated production of the lightest chargino, $\widetilde{\chi}_1^\pm$, and the next to lightest neutralino, $\widetilde{\chi}_2^0$, decaying into three leptons and missing transverse energy leads to a clean signature with low standard model background. This final state under consideration is referred to the trilepton channel. The associated production of the $\widetilde{\chi}_1^\pm$ and $\widetilde{\chi}_2^0$ takes place via an off-shell W boson in the s channel or a squark exchange in the t channel. The corresponding graphs are presented in Figure 1. As illustrated in Figure 2, $\widetilde{\chi}_1^\pm$ and $\widetilde{\chi}_2^0$ decay into a lepton accompanied by a particle escaping detection (neutrino or LSP) through virtual gauge boson or sleptons.

Figure 1: Graphs for $\widetilde{\chi}_1^\pm/\widetilde{\chi}_2^0$ pair production.

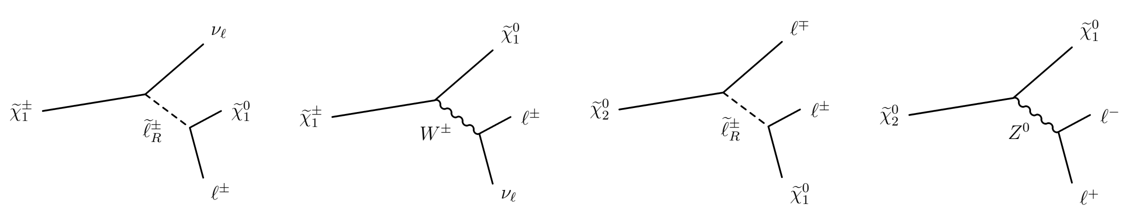

Figure 2: Graphs for $\widetilde{\chi}_1^\pm$ and $\widetilde{\chi}_2^0$ decays in leptonic final states.

The leptonic decays of $\widetilde{\chi}_1^\pm$ and $\widetilde{\chi}_2^0$ lead to a final state with three leptons and missing transverse energy. For a given set of parameters in the mSUGRA space, the third lepton may be very soft, especially if the mass difference between $\widetilde{\chi}_2^0$ and $\widetilde{\ell}_R$ is small. Distributions of the transverse momentum for both the three leptons and like sign pair are displayed in Figure 3.

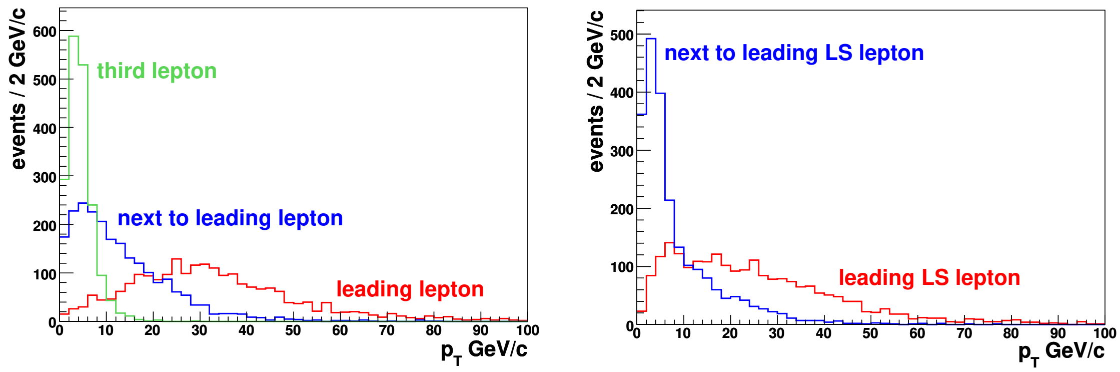

Figure 3: Distributions, at the generator level, of the tranverse momentum (p_T) for the leptons coming from the process $\widetilde{\chi}_1^{\pm}\widetilde{\chi}_2^0 \rightarrow 3\ell$ considering the three leptons (left) and only the like sign pair (right). Leptons are sorted with respect to their p_T. mSUGRA parameters are $m_0 = 72$ GeV/c^2, $m_{1/2} = 175$ GeV/c^2, $\tan\beta = 3$, $A_0 = 0$ GeV/c^2 and $\mu > 0$ corresponding to the following masses: $m_{\widetilde{\ell}_R} = 104.4$ GeV/c^2, $m_{\widetilde{\chi}_2^0} = 112.4$ GeV/c^2.

Previous searches at DØ have set limits on the associated production of $\widetilde{\chi}_1^{\pm}\widetilde{\chi}_2^0$ [6]. Since most of the selections are relying on the reconstruction of all three leptons, efficiencies for points with small mass difference between $\widetilde{\ell}_R$ and $\widetilde{\chi}_2^0$ are very low. Therefore, a like sign leptons signature has been developed to deal with such a topology. Search for supersymmetry in the like sign dimuon channel is presented hereafter.

2 Data samples

The selection is based on data collected from April 2002 up to February 2006 by the DØ detector at the Fermilab Tevatron collider at a center of mass energy of 1.96 TeV and corresponds to an integrated luminosity of 902 ± 59 pb^{-1}. All simulated signal and standard model processes are generated with `Pythia 6.323` [7] and processed through the full detector simulation. Masses of $\widetilde{\chi}_1^{\pm}$ beyond LEP limit of 103.5 GeV/c^2 [8] are under consideration. The signal points used to optimize the selection correspond to a choice of $m_{\widetilde{\ell}_R} \lesssim m_{\widetilde{\chi}_2^0}$. The two body decay $\widetilde{\chi}_2^0 \rightarrow \widetilde{\ell}_R^{\pm}\ell^{\mp}$ is then enhanced, leading to final states with a very soft third lepton. The other mSUGRA parameters are set to the following values: $\tan\beta = 3$, $A_0 = 0$ GeV/c^2 and $\mu > 0$. A detailed description of the generated points is given in Table 1. The major background for the like sign dimuon signature comes from multijet background from QCD processes, mostly $b\bar{b}$. Muons are therefore expected to be produced in association with jets. Real data events with non isolated muons are selected in order to estimate the multijet background.

point	m_0 GeV/c^2	$m_{1/2}$ GeV/c^2	$m_{\widetilde{\chi}_2^0}$ GeV/c^2	$m_{\widetilde{\chi}_1^\pm}$ GeV/c^2	$m_{\widetilde{\ell}_R}$ GeV/c^2	$m_{\widetilde{\tau}_1}$ GeV/c^2	$\sigma_{\mathrm{NLO}} \times BR(3\ell)$ fb
B2	68	170	108.2	104.3	100.6	99.2	838±7
C2	72	175	112.4	108.9	104.4	103.1	713±6
D2	76	180	116.7	113.3	108.4	107.0	596±4
E2	80	185	120.9	117.7	112.3	111.0	511±4
F2	98	205	138.0	135.6	129.8	128.7	180±3

Table 1: Values of m_0 and $m_{1/2}$ parameters for the generated points. The other parameters are set to the following values: $\tan\beta = 3$, $A_0 = 0$ GeV/c^2 and $\mu > 0$. The masses of $\widetilde{\chi}_2^0$, $\widetilde{\chi}_1^\pm$, $\widetilde{\ell}_R$, $\widetilde{\tau}_1$ and the cross-section times branching fraction into three leptons are also indicated.

3 Event selection

Events firing a set of dimuon triggers with p_T threshold close to 5 GeV/c are selected. In order to reject badly reconstructed objects, events with two like sign muon candidates matched to a central track with $p_T > 5$ GeV/c are selected. The background is dominated by muons from b-decays which are less isolated than muons from signal. In the following, the muon isolation is defined by the nearby activity around the muon candidate in the calorimeter and/or tracker. Two muon isolation criteria are considered.

muon tight isolated:

- $E_T^{0.1<\Delta R<0.4} < 2.5$ GeV
- $p_T^{\Delta R<0.5} < 2.5$ GeV/c

muon loose isolated:

- $E_T^{0.1<\Delta R<0.4} < 4$ GeV
- $p_T^{\Delta R<0.5} < 4$ GeV/c

where $E_T^{0.1<\Delta R<0.4}$ stands for the sum of the energy depositions in all the calorimeter cells lying in a calorimeter hollow cone with inner and outer radii respectively set to $R_{inner} = 0.1$ and $R_{outer} = 0.4$ and $p_T^{\Delta R<0.5}$ stands for the transverse momentum sum of all the tracks (excluding the muon candidate) lying in a tracker cone with radius $R = 0.5$. All cones are centered around the muon candidate direction. ΔR is defined as $\Delta R = \sqrt{\Delta\eta^2 + \Delta\varphi^2}$ with $\Delta\eta$ and $\Delta\varphi$ respectively the distance in pseudo-rapidity and the angular difference in the plane transverse to the beam direction. To reduce further the muons from b-decays, both muons are required to come from the primary vertex within 1 cm along the beam direction. Due to the multijet background estimation procedure, a cut on the angular distance in the transverse plane between the like sign muons, $\Delta\varphi(\mu,\mu) < 2.9$, is added. This set of cuts is referred to the selection $\mathcal{A}$. Several additional cuts are studied in order to extract the signal from the background.

Missing transverse energy:

The $\widetilde{\chi}_1^0$ produced in $\widetilde{\chi}_1^\pm$ and $\widetilde{\chi}_2^0$ decays is stable and escapes detection leading to a significant amount of missing transverse energy. In addition, for events with jets with transverse energies above 15 GeV, a cut on the significance Sig($\not\!\!E_T$) is used. The Sig($\not\!\!E_T$) is defined by normalizing the $\not\!\!E_T$ to $\sigma(E_T^j \,\|\not\!\!E_T)$, a measure of the jet energy resolution projected onto the $\not\!\!E_T$ direction:

$$\mathrm{Sig}(\not\!\!E_T) = \frac{\not\!\!E_T}{\sqrt{\sum_{\mathrm{jets}} \sigma^2_{E_T^j \| \not E_T}}}.$$

The distributions of both missing transverse energy and Sig($\not\!\!E_T$) for data, signal and background processes are presented in Figure 4.

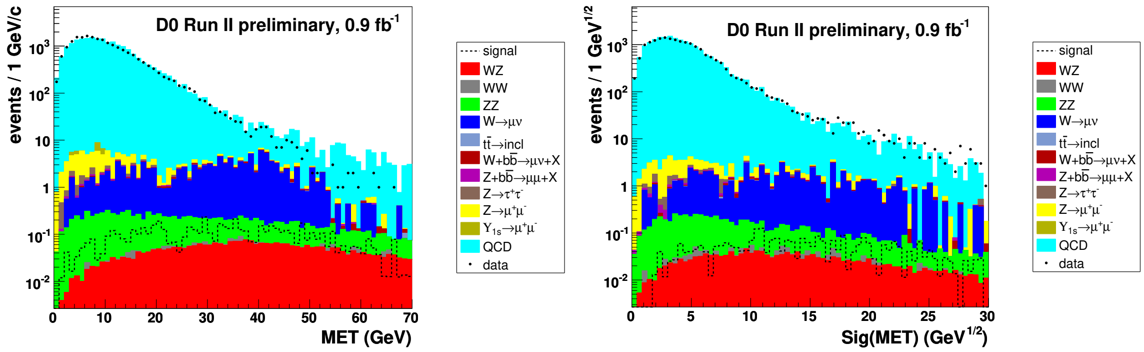

Figure 4: Distributions of the missing transverse energy (left) and Sig($\not\!\!E_T$) (right) observed in data and expected for the background and signal. The selection $\mathcal{A}$ is applied.

Invariant masses:

Cuts on the invariant masses of opposite signs and like sign dimuon pairs have been studied in order to reduce respectively the contribution of background events with a Z boson decaying into two opposite signs muons and multijet background which is expected in the low mass region. A cut on the transverse mass made with the missing transverse energy and the next to leading muon p_T is also used to reject events from W and diboson background processes. The distributions of these variables are displayed in Figure 5.

Momenta:

Cuts on the muon momenta have been optimized to optimally reject the multijet background. The distributions of the transverse momentum for the leading muon, next to leading muon and like sign dimuon pair and the distribution of the missing transverse energy times the next to leading muon p_T are presented in Figure 6.

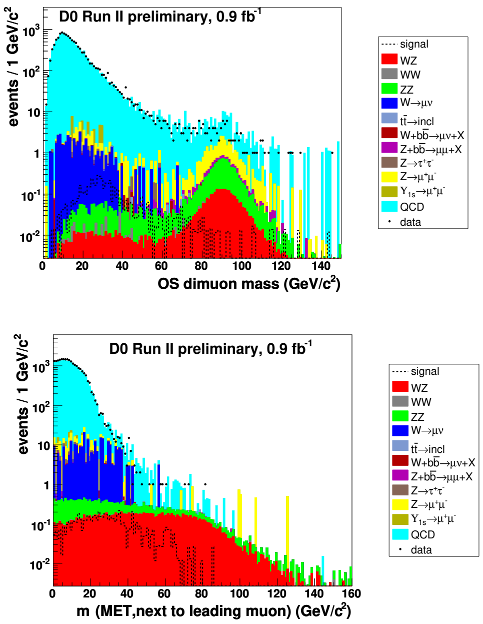

Figure 5: Distributions of the invariant masses of opposite signs (top left) and like sign (top right) muon pairs and of the transverse mass made with the missing transverse energy and the next to leading muon p_T (bottom left) observed in data and expected for the background and signal. The selection $\mathcal{A}$ is applied.

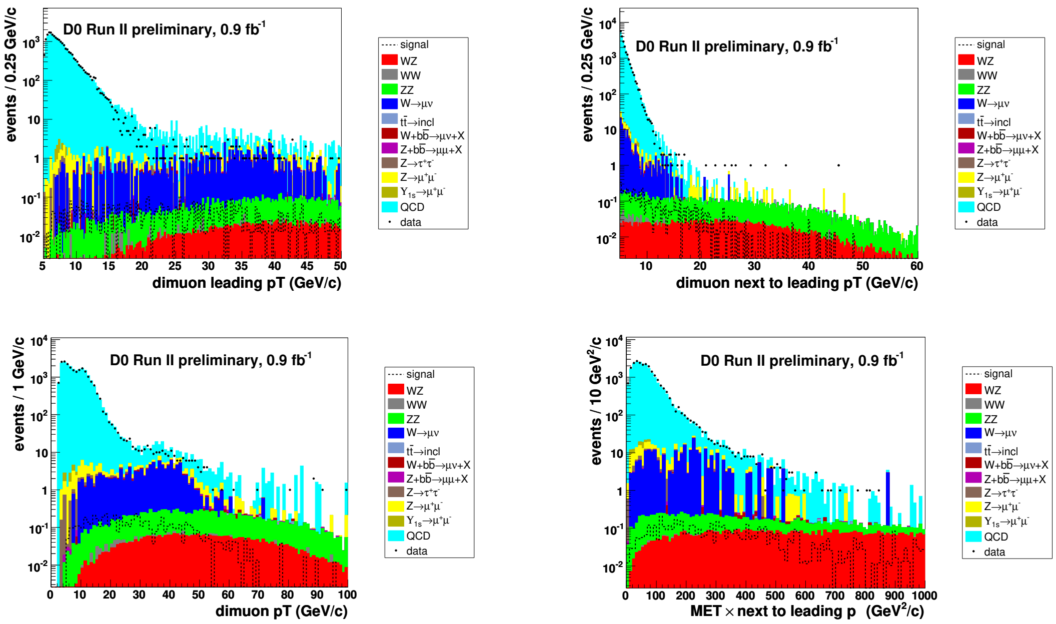

Figure 6: Distributions of the transverse momentum for the leading muon (top left), next to leading muon (top right) and like sign dimuon pair (bottom left) and of the missing transverse energy times the next to leading muon p_T (bottom right) observed in data and expected for the background and signal. The selection $\mathcal{A}$ is applied.

Those criteria have been optimized to get the best expected limit on the quantity $\sigma(p\bar{p} \to \widetilde{\chi}_1^{\pm}\widetilde{\chi}_2^0) \times BR(3\ell)$ using the modified frequentist approach defined in the reference [10] with a special emphasis on topologies with a very soft third lepton. The point C2 ($m_0 = 72$ GeV/c^2, $m_{1/2} = 175$ GeV/c^2, $\tan\beta = 3$, $A_0 = 0$ GeV/c^2 and $\mu > 0$) has been used to perform the optimization and the results are summarized in Table 2.

	criteria
a	$M_{\mu^{\pm}\mu^{\mp}}$ ϵ [25 − 70] GeV/c^2 if opposite signs pairs are reconstructed
b	$p_T^{\mu^2} < 35$ GeV/c
c	$p_T^{\mu^2} > 8$ GeV/c
d	$p_T^{\mu^1} > 13$ GeV/c
e	$M_{\mu^{\pm}\mu^{\pm}}$ ϵ [12 − 110] GeV/c^2
f	$M_T(\not\!\!E_T, p_T^{\mu^2})$ ϵ [15 − 65] GeV/c^2
g	$\not\!\!E_T > 10$ GeV
h	Sig($\not\!\!E_T$) > 12 GeV$^{1/2}$
i	$\not\!\!E_T \times p_T^{\mu^2} > 160$ GeV^2/c

Table 2: Summary of selection criteria obtained after optimization.

4 Results

The number of events expected for background processes and observed in data after each step of the selection is listed in Table 3. The single event observed in data is consistent with the 1.1±0.4 events expected from background. The number of expected events and the efficiencies for the signal at different levels of cuts are presented in Table 4. A limit on the quantity $\sigma(p\bar{p} \to \widetilde{\chi}_1^{\pm}\widetilde{\chi}_2^0) \times BR(3\ell)$ has been derived. When $m_{\widetilde{\ell}_R} \lesssim m_{\widetilde{\chi}_2^0}$ (so called points B2, C2, D2, E2 and F2), the like sign dimuon selection plays a major role due to the softness of the third lepton. Observed and expected limits considering those points are presented in Figure 7 as a function of $\widetilde{\chi}_1^{\pm}$ mass. The region above the curve is excluded at 95% CL using the modified frequentist approach defined in the reference [10].

	cut	QCD	WZ	ZZ	$W \rightarrow \mu\nu$	$Z \rightarrow \mu^+\mu^-$
$\mathcal{A}$	preselection	14787±981	3.3±0.2	9.7±0.7	58±7	42±5
a	$M_{\mu^\pm\mu^\mp}$ ϵ [25 − 65] GeV/c^2	3452±232	0.66±0.05	0.70±0.06	16±3	4.2±1.0
b	$p_T^{\mu_2}$ < 35 GeV/c	3452±232	0.53±0.04	0.64±0.06	16±3	4.2±1.0
c	$p_T^{\mu_2}$ > 10 GeV/c	4.9±1.5	0.42±0.03	0.43±0.04	1.9±0.9	0.4±0.2
d	$p_T^{\mu_1}$ > 13 GeV/c	2.8±1.1	0.41±0.03	0.42±0.04	1.9±0.9	0.4±0.2
e	$M_{\mu^\pm\mu^\pm}$ ϵ [12 − 110] GeV/c^2	1.4±0.7	0.39±0.03	0.38±0.04	1.9±0.9	0.4±0.2
f	$M_T(\not\!\!E_T, p_T^{\mu_2})$ ϵ [15 − 65] GeV/c^2	0.9±0.5	0.32±0.02	0.32±0.04	0.7±0.5	0.4±0.2
g	$\not\!\!E_T$ > 10 GeV	0.5±0.3	0.30±0.02	0.27±0.03	0.7±0.5	0.3±0.2
h	Sig($\not\!\!E_T$) > 12 GeV$^{1/2}$	0.19±0.19	0.198±0.015	0.16±0.02	0.7±0.5	0.21±0.14
i	$\not\!\!E_T \times p_T^{\mu_2}$ > 160 GeV^2/c	0.19±0.19	0.194±0.015	0.16±0.02	0.2±0.2	0.21±0.14

		Wbb	Zbb	WW	sum	data
$\mathcal{A}$	preselection	3.2±0.3	2.5±0.2	0.14±0.02	14922±981	15234
a	$M_{\mu^\pm\mu^\mp}$ ϵ [25 − 65] GeV/c^2	0.37±0.06	2.3±0.3	0.13±0.03	3486±233	3569
b	$p_T^{\mu_2}$ < 35 GeV/c	0.35±0.06	2.3±0.3	0.13±0.03	3479±232	3358
c	$p_T^{\mu_2}$ > 10 GeV/c	0.09±0.03	0.21±0.07	0.026±0.009	8.9±1.8	10
d	$p_T^{\mu_1}$ > 13 GeV/c	0.08±0.03	0.21±0.07	0.026±0.009	6.5±1.4	6
e	$M_{\mu^\pm\mu^\pm}$ ϵ [12 − 110] GeV/c^2	0.07±0.02	0.21±0.07	0.023±0.009	5.1±1.2	2
f	$M_T(\not\!\!E_T, p_T^{\mu_2})$ ϵ [15 − 65] GeV/c^2	0.06±0.02	0.19±0.07	0.013±0.006	2.9±0.8	2
g	$\not\!\!E_T$ > 10 GeV	0.05±0.02	0.19±0.07	0.006±0.003	2.3±0.7	1
h	Sig($\not\!\!E_T$) > 12 GeV$^{1/2}$	0.03±0.015	0.16±0.06	0.006±0.003	1.7±0.6	1
i	$\not\!\!E_T \times p_T^{\mu_2}$ > 160 GeV^2/c	0.02±0.014	0.16±0.06	0.006±0.003	1.1±0.4	1

Table 3: Number of events expected from background processes and observed in data at the different levels of the selection.

	cut	B2	C2	D2	E2	F2
$\mathcal{A}$	preselection	8.4±0.6	7.4±0.6	6.2±0.5	5.6±0.4	3.0±0.2
a	$M_{\mu^\pm\mu^\mp}$ ϵ [25 − 65] GeV/c^2	7.9±0.6	6.9±0.5	5.7±0.4	5.3±0.4	2.7±0.2
b	$p_T^{\mu_2}$ < 35 GeV/c	7.6±0.6	6.6±0.5	5.4±0.4	5.2±0.4	2.49±0.19
c	$p_T^{\mu_2}$ > 10 GeV/c	6.4±0.5	5.8±0.5	4.7±0.4	4.9±0.4	2.12±0.14
d	$p_T^{\mu_1}$ > 13 GeV/c	5.8±0.5	5.2±0.4	4.2±0.3	4.2±0.3	2.00±0.16
e	$M_{\mu^\pm\mu^\pm}$ ϵ [12 − 110] GeV/c^2	5.7±0.5	5.2±0.4	4.2±0.3	4.2±0.3	2.00±0.16
f	$M_T(\not\!\!E_T, p_T^{\mu_2})$ ϵ [15 − 65] GeV/c^2	5.4±0.4	5.0±0.4	4.0±0.3	3.8±0.3	1.90±0.13
g	$\not\!\!E_T$ > 10 GeV	4.8±0.4	4.7±0.4	3.6±0.3	2.9±0.2	1.59±0.13
h	Sig($\not\!\!E_T$) > 12 GeV$^{1/2}$	4.6±0.4	4.4±0.3	3.4±0.3	2.6±0.2	1.51±0.13
i	$\not\!\!E_T \times p_T^{\mu_2}$ > 160 GeV^2/c	4.0±0.4	4.0±0.3	2.9±0.3	2.4±0.2	1.33±0.12

	cut	B2	C2	D2	E2	F2
$\mathcal{A}$	preselection	26.0±1.0	27.5±1.0	28.2±1.0	26.7±1.0	30.4±1.1
a	$M_{\mu^\pm\mu^\mp}$ ϵ [25 − 70] GeV/c^2	24.5±1.0	25.6±1.0	25.8±1.0	25.4±0.9	27.5±1.0
b	$p_T^{\mu_2}$ < 35 GeV/c	23.5±0.9	24.5±1.0	24.8±1.0	24.7±0.9	25.3±1.0
c	$p_T^{\mu_2}$ > 10 GeV/c	20.0±0.9	21.3±0.9	21.3±0.9	23.4±0.9	21.6±0.9
d	$p_T^{\mu_1}$ > 13 GeV/c	18.0±0.9	19.3±0.9	19.2±0.9	20.3±0.9	20.4±0.9
e	$M_{\mu^\pm\mu^\pm}$ ϵ [12 − 110] GeV/c^2	17.8±0.8	19.1±0.9	19.1±0.9	20.3±0.9	20.4±0.9
f	$M_T(\not\!\!E_T, p_T^{\mu_2})$ ϵ [15 − 65] GeV/c^2	16.7±0.8	18.4±0.8	18.2±0.9	17.9±0.8	19.4±0.9
g	$\not\!\!E_T$ > 10 GeV	15.0±0.8	17.5±0.8	16.5±0.8	13.8±0.7	16.3±0.9
h	Sig($\not\!\!E_T$) > 12 GeV$^{1/2}$	14.4±0.8	16.5±0.8	15.5±0.8	12.3±0.7	15.6±0.8
i	$\not\!\!E_T \times p_T^{\mu_2}$ > 160 GeV^2/c	12.5±0.7	14.8±0.8	13.4±0.8	11.5±0.7	13.7±0.8

Table 4: Number of events (top) and efficiencies in % (bottom) expected from signal according the different levels of selection. Sets of mSUGRA parameters defined in Table 1 are under consideration.

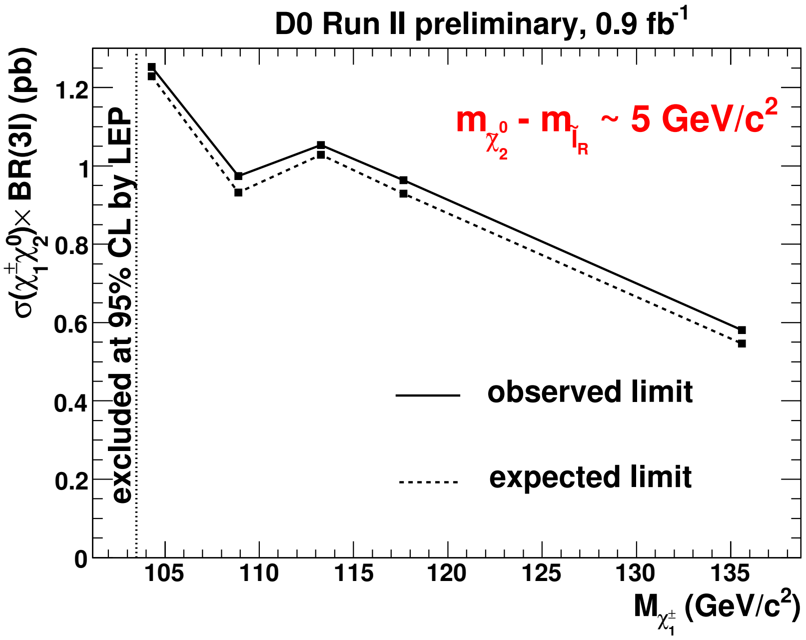

Figure 7: Observed limit for $\sigma(p\bar{p} \to \widetilde{\chi}_1^\pm \widetilde{\chi}_2^0) \times BR(3\ell)$ for $m_{\widetilde{\ell}_R} \lesssim m_{\widetilde{\chi}_2^0}$ mSUGRA points. The $\widetilde{\chi}_1^\pm$ mass region below 103.5 GeV/c^2 is excluded by LEP search [11]. The region above the curve is excluded at 95% CL. The squares correspond to the five mSUGRA points defined in Table 1

5 Conclusion

A search for the associated production of $\widetilde{\chi}_1^\pm$ and $\widetilde{\chi}_2^0$ in like sign dimuon channel using a dataset corresponding to an integrated luminosity of 902±59 pb^{-1} has been performed. The selection has been optimized in order to obtain the best expected limit on the quantity $\sigma(p\bar{p} \to \widetilde{\chi}_1^\pm \widetilde{\chi}_2^0) \times BR(3\ell)$. The observation of one event in the data is consistent with the 1.1±0.4 events expected from the background. A limit has been derived from the results.

Acknowledgement

We thank the staffs at Fermilab and collaborating institutions, and acknowledge support from the DOE and NSF (USA);CEA and CNRS/IN2P3 (France);FASI, Rosatom and RFBR (Russia);CAPES, CNPq, FAPERJ, FAPESP and FUNDUNESP (Brazil);DAE and DST (India);Colciencias (Colombia);CONACyT (Mexico);KRF and KOSEF (Korea);CONICET and UBACyT (Argentina);FOM (The Netherlands); PPARC (United Kingdom);MSMT (Czech Republic);CRC Program, CFI, NSERC and WestGrid Project (Canada);BMBF and DFG (Germany);SFI (Ireland);The Swedish Research Council (Sweden);Research Corporation;Alexander von Humboldt Foundation;and the Marie Curie Program.

References

[1] H. Nilles, *Supersymmetry supergravity and particle physics*, Phys. Rep. **110** (1984) 1; H. Haber et G. Kane, *The search for supersymmetry: probing physics beyond the standard model*, Phys. Rep. **117** (1985) 75.

[2] S. Dawson, *The MSSM and why it works*, BNL-HET-SD-97-4 (1997), hep-ph/9712464.

[3] L. Hall, J. Lykken et S. Weinberg, *Supergravity as the messenger of supersymmetry breaking*, Phys. Rev. **D27** (1983) 2359.

[4] S. Dawson, *R-parity breaking in supersymmetric theories*, Nucl. Phys. **261** (1985) 297.

[5] W. Beenakker *et al.*, *The production of charginos/neutralinos and sleptons at hadron colliders*, Phys. Rev. Lett. **83** (1997) 3780, hep-ph/9906298.

[6] DØ Collaboration, *Search for supersymmetry via associated production of charginos and neutralinos in final states with three leptons*, Fermilab-Pub-05-075-E, Phys. Rev. Lett. **95** 151805 (2005), hep-ex/0504032.

[7] T. Sjö̈strand, Comp. Phys. Commun. **82** (1994) 74.

[8] LEPSUSYWG, ALEPH, DELPHI, L3 and OPAL experiments, *Charginos, large* m_0 LEPSUSYWG/01-03.1 (lepsusy.web.cern.ch/lepsusy/Welcome.html).

[9] W. Porod, Comp. Phys. Commun. **153** (2003) 275.

[10] T. Junk, *Confidence level computation for combining searches with small statistics*, Nucl. Instrum. Meth. **A434** (1999) 435; V. Büescher *et al.*.

[11] LEPSUSYWG, ALEPH, DELPHI, L3 and OPAL experiments, *Charginos, large* m_0 LEPSUSYWG/01-03.1 (lepsusy.web.cern.ch/lepsusy/Welcome.html).